Measurement of the refractive indices of KDP and ADP at low temperatures

Grace Wu

Pittsford Mendon High School

Pittsford, NY

Advisor: Ildar Begishev

Laboratory for Laser Energetics

University of Rochester

Rochester, NY

April 2023

1 Abstract

Potassium dihydrogen phosphate (KDP) and ammonium dihydrogen phosphate (ADP) are nonlinear optical crystals used to convert radiation of high-power, large-aperture infrared lasers into the deep-ultraviolet range. The current temperature-dependent Sellmeier equations for both KDP and ADP don't correspond to experimental data at low temperatures. In this work the refractive indices of KDP and ADP were measured at different temperatures to allow the equations to be modified. Initially, the refractive indices of both crystals were measured at room temperature and checked by comparison with existing values. Prisms from KDP and ADP crystals were then placed inside a two-chamber cryostat, and two laser beams of different wavelengths (633 nm and 533 nm) were aligned to the prisms. Liquid nitrogen was pumped into the cryostat, cooling the crystals down from approximately 300 K to 200 K. The refractive indices were measured for ordinary and extraordinary beams based on the positions of the refracted beams as the temperature changed. The experimental data were fitted to new equations, which were then compared with the original equations.

2 Introduction

Nonlinear crystals are often used in lasers and electro-optical applications, including the OMEGA [1] and OMEGA EP [2] lasers at the Laboratory for Laser Energetics of the University of Rochester. Currently, the most powerful lasers emit light in the infrared range. However, many applications, such as high-density plasma diagnostics [3], require high-energy deep ultraviolet (UV) sources. Unfortunately, only a few lasers can generate UV light directly. They either cannot provide sufficiently energetic beams in the UV region, or they are too complicated (excimer laser) [4]. Methods of nonlinear optics can be utilized to convert infrared light into UV. Particularly, the

fifth-harmonic generation (FHG) of large-aperture neodymium lasers in ADP and KDP can provide beams with high UV energies due to the availability of large ADP and KDP crystals. Harmonics are laser beams with a frequency that is n-times higher than the fundamental (initial) laser frequency of ω, where n is an integer and ω is the circular frequency of the light. The simplest example is second harmonic generation (SHG), where two photons at the fundamental ω generate one photon of second harmonic with frequency 2ω: $\omega + \omega = 2\omega$.

Another type of nonlinear process is frequency mixing. For example, the third harmonic generation (THG) process $\omega + 2\omega = 3\omega$ provides photons of the third harmonic from photons of the second harmonic, 2ω, and residual photons of fundamental frequency ω left after SHG. THG is used on all 60 beams of the OMEGA laser to convert radiation with a wavelength of 1054 nm into UV light with a wavelength of 351 nm. The fourth harmonic generation can be generated in a cascade of two SHG processes. Finally, the FHG can be realized in a cascade of three processes:

$$\omega + \omega = 2\omega \;>\; 2\omega + 2\omega = 4\omega \;>\; \omega + 4\omega = 5\omega$$

To convert light of one wavelength into another, it is necessary to match their phase velocity in a crystal. Nonlinear crystals can achieve this because of the birefringence effect, which can split light into two different beams inside the crystals, the ordinary and extraordinary. At orthogonal polarizations, these beams can have the same refractive index and therefore the same phase velocity for different wavelengths. This process is called phase matching and can only be achieved in a certain beam direction inside a crystal. Since the angular acceptance range for the direction is very small, it could be called critical angular phase matching. Thus, we can generate the second harmonic $\omega + \omega = 2\omega$, where ω is the ordinary beam and 2ω is the extraordinary beam. Both beams have the same refractive index, but in orthogonal polarizations. As a result, we can

efficiently convert 1054 nm light into 527 nm light. Second, in a similar process in a cascade, we can generate the fourth harmonic: $2\omega + 2\omega = 4\omega$, with the resulting wavelength at 264 nm. To generate light at 211 nm, we must realize the $\omega + 4\omega = 5\omega$ process. This can be written in vector form as

$$k_1{}^o + k_4{}^o = k_5{}^e$$

where $k_i{}^{o,e} = \frac{2\pi}{\lambda_i} n^{o,e}$ are the wave vectors for different harmonics i and ordinary (o) or extraordinary (e) beams with λ_i the vacuum wavelength of harmonic i.

Interaction beams can be non-collinear. In our case of FHG, all beams are collinear. The phase matching for FHG can be realized when

$$\Delta k = k_5{}^e - k_1{}^o - k_4{}^o = 0 \quad (1)$$

This can't be achieved at room temperature in ADP and KDP, but we can tune the refractive indices of these crystals by changing the temperature and reaching the phase matching condition (1). Moreover, when the angle between the direction of beam propagation in a crystal and the z-axis of a crystal is close to 90°, the angle tolerance is less tight. In this case, the phase matching (1) is said to be noncritical.

Noncritical phase matching for ($\omega + 4\omega$) was achieved by cooling an ADP or KDP large-aperture crystal in a two-chamber cryostat [5] below 200 K. While the total conversion efficiency from the fundamental to the fifth harmonic at 211 nm was 26% using ADP [5], there was a significant discrepancy between the calculated (230 K) and experimentally measured (200 K) temperatures of noncritical phase matching. This likely comes from incorrect refractive indices *n*

of crystals at low temperatures. Currently, there are not many available *n* measurements at low temperatures, so it is necessary to accurately measure *n* of ADP and KDP crystals at low temperatures.

As a result of the birefringence of KDP and ADP, double refraction occurs when a beam is put through the crystal a certain way. If there are two polarizations coming into a nonlinear crystal, the horizontal and vertical, the beam is split into the ordinary and extraordinary beams. These beams propagate with different angles because they have different velocities in the material, as shown in Figure 1.

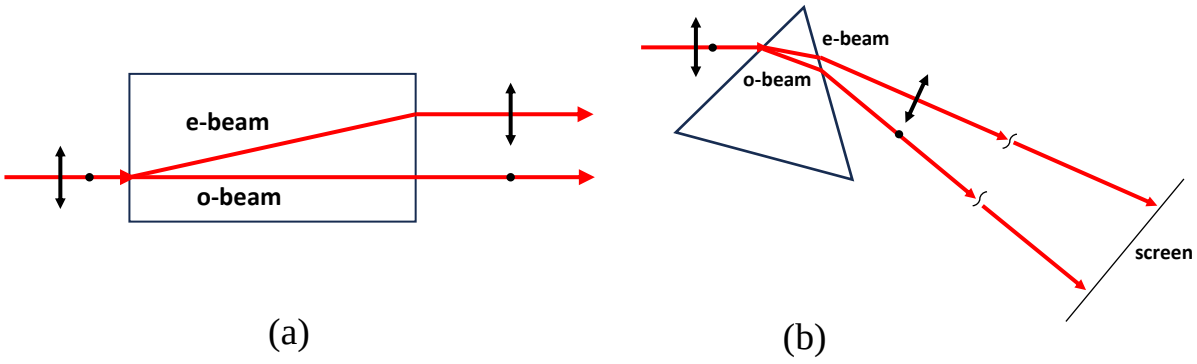

Figure 1: Ordinary (o) and extraordinary (e) beams for rectangular and triangular prisms. Figure 1a shows a rectangular prism, and the two beams come out parallel to each other, but with the e-beam displaced sideways. Figure 1b shows a triangular prism, and the two beams diverge at an angle. The screen allows the position of the refracted beams to be tracked and measured.

Temperature-dependent Sellmeier equations (2) relate refractive index to temperature and wavelength for KDP and ADP [6]. Based on the original temperature-dependent Sellmeier equations, we calculated the temperature when non-critical phase matching of the $\omega + 4\omega = 5\omega$ process should occur. However, it was different from the experimentally measured

temperature. Since Equations (2) don't match experimental data at low temperatures, they need to be modified.

KDP:

$$n_o{}^2 = (1.44896 + 3.185 * 10^{-5}T) + \frac{(0.84181 - 1.4114 * 10^{-4}T) * \lambda^2}{\lambda^2 - (0.0128 - 2.13 * 10^{-7}T)} + \frac{(0.90793 + 5.75 * 10^{-8}T) * \lambda^2}{\lambda^2 - 30}$$

$$n_e{}^2 = (1.42691 - 1.152 * 10^{-5}T) + \frac{(0.72722 - 6.139 * 10^{-5}T) * \lambda^2}{\lambda^2 - (0.01213 + 3.104 * 10^{-7}T)} + \frac{(0.22543 - 1.98 * 10^{-7}T) * \lambda^2}{\lambda^2 - 30}$$

(2)

ADP:

$$\mathrm{n_o}{}^2 = (1.6996 - 8.7835 * 10^{-4}\mathrm{T}) + \frac{(0.64955 + 7.2007 * 10^{-4}\mathrm{T}) * \lambda^2}{\lambda^2 - (0.01723 - 1.40526 * 10^{-5}\mathrm{T})} + \frac{(1.10624 - 1.179 * 10^{-4}\mathrm{T}) * \lambda^2}{\lambda^2 - 30}$$

$$n_e{}^2 = (1.6996 - 8.7835 * 10^{-4}T) + \frac{(0.64955 + 7.2007 * 10^{-4}T) * \lambda^2}{\lambda^2 - (0.01723 - 1.40526 * 10^{-5}T)} + \frac{(1.10624 - 1.179 * 10^{-4}T) * \lambda^2}{\lambda^2 - 30}$$

where T is the temperature in K and λ is wavelength in μm.

In this work, two prisms of ADP and KDP were fabricated. An automated system for continuous filling of the existing two-chamber cryostat [5] by liquid nitrogen was designed and built. The refractive indices were checked at room temperature first. Then, the crystalline prisms were moved into a cryostat where the temperature could be lowered using a liquid nitrogen system. The refractive indices of KDP and ADP were measured using the deviation of the ordinary and extraordinary beams.

3 Experimental Setup

3.1 Room Temperature Testbed

In a rectangular crystal, the ordinary and extraordinary beams come out of the crystal parallel and close to each other, as shown in Figure 1a. To better differentiate between the two refracted beams, the crystals were cut into triangular prisms, as shown in Figure 1b. Using a rotating stage, the tip angles of both prisms were measured. This is the angle p between the input and output surfaces of the prisms (see Fig. 2). The KDP prism has an angle of 46.33° and the ADP prism has an angle of 43.98°.

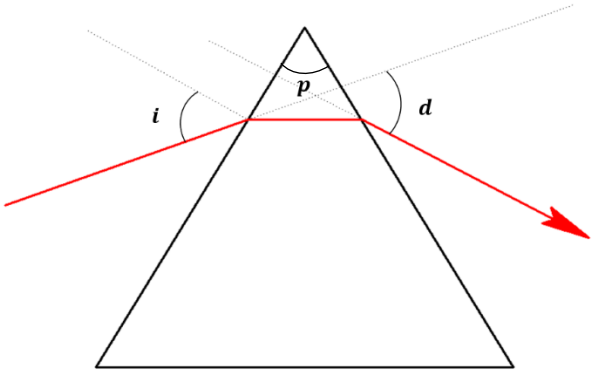

Figure 2: Diagram showing a beam refracting through a prism. The angle of deviation d can be determined from the incidence angle i, the prism angle p, and the refractive index of the crystal.

To begin, measurements were made at room temperature to ensure that the measurements matched with the existing values for the refractive indices of KDP and ADP. For this experiment, a testbed was assembled at room temperature. A red helium-neon (He-Ne) laser and a green semiconductor laser were used to measure the refractive indices at these two different wavelengths of light. Using a spectrophotometer, the red laser was determined to have a wavelength of 633 nm and the green laser to have a wavelength of 533 nm. The beams were put through the prisms at an incidence angle of 8° for ADP and 12° for KDP. The angle of deviation (see Fig. 2), which is how

much a beam changes as it goes through the prism, was measured for KDP and ADP at room temperature. The angles for ADP were measured to be 31.21°, 36.27°, 31.46°, and 36.94° for the extraordinary red beam, ordinary red beam, extraordinary green beam, and ordinary green beam, respectively. Similarly, the angles for KDP were measured to be 35.40°, 43.45°, 35.30°, and 43.22° for the extraordinary red beam, ordinary red beam, extraordinary green beam, and ordinary green beam, respectively. The theoretical values were determined by

$$d = sin^{-1}\left[n\, sin(p - \sin^{-1}(\frac{\sin i}{n}))\right] + i - p \quad (3)$$

where d is the angle of deviation, i is the angle of incidence, n is the refractive index, and p is the angle of the prism.

Using the diagram in Figure 2, Equation (3) was derived using Snell's law and geometry. Snell's Law states that $n_1 \sin\theta_1 = n_2 \sin\theta_2$, where n_1 and θ_1 are the refractive index and incident angle of the first material, respectively, and n_2 and θ_2 are the refractive index and refracted angle of the second material, respectively. Experimental values for ADP were compared to the theoretical angles of deviation at room temperature, which are 31.12°, 36.26°, 31.55°, and 37.00°, respectively. The theoretical values for KDP are 35.45°, 43.42°, 35.99°, and 45.02°. Since the theoretical and experimental values for the angle of deviation closely matched for both prisms, the next step was making the measurements at low temperatures.

3.2 Two-Chamber Cryostat

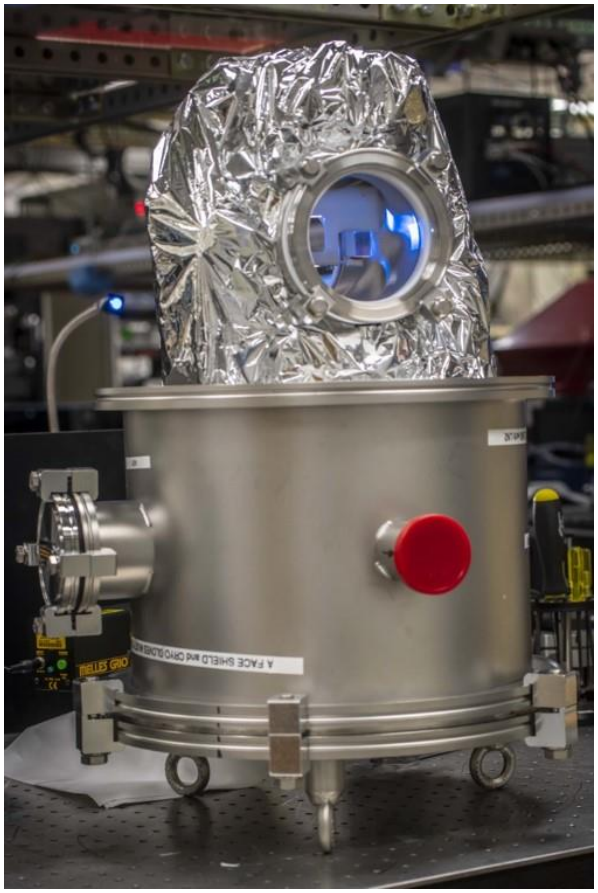

Figure 3: Unassembled two-chamber cryostat with prisms inside. The crystals are placed inside the internal chamber, which is insulated by mylar-aluminum foil. The cryostat is inverted in this figure because it was in the process of being assembled.

The two-chamber cryostat, shown in Figure 3, is made up of external and internal chambers. The internal chamber contains a crystal mount, which was 3-D printed to fit the KDP and ADP crystals. Temperature and pressure sensors were placed on the mount to record the temperatures of the crystals and ensure that the pressure inside the chamber is stable. The mount with ADP and KDP prisms and temperature and pressure sensors is shown in Figure 4.

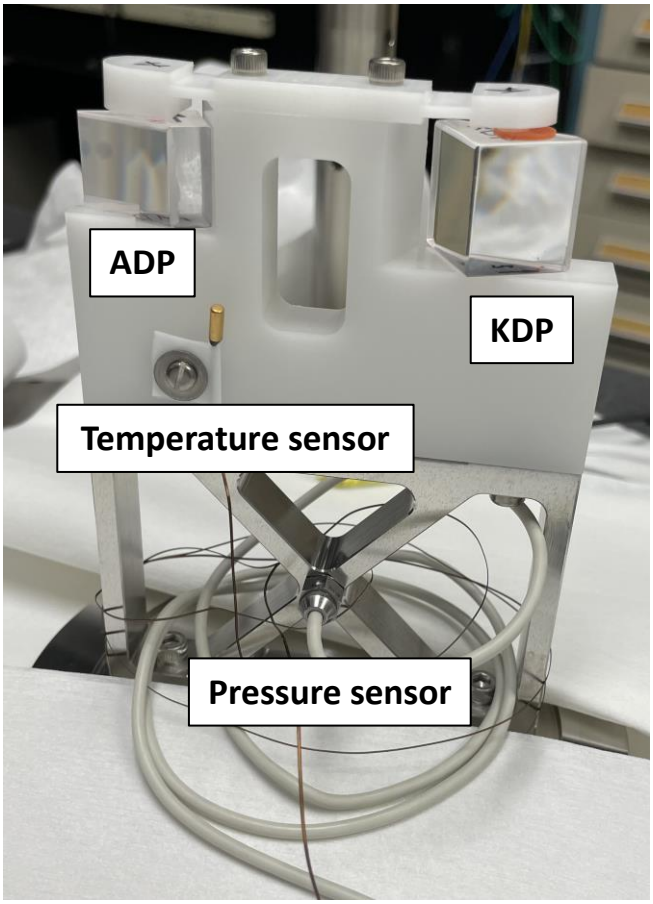

Figure 4: ADP and KDP crystals inside the 3D-printed mount. There are temperature and pressure sensors on the mount to track the temperature and ensure that the pressure inside the internal chamber is stable.

The internal chamber is filled with 1 atm of helium, which was chosen due to its high thermal conductivity. A liquid nitrogen tank is located inside the external chamber and connected to the internal chamber. “Cold flow” goes from the liquid nitrogen tank into the internal chamber. Since the contact area between the prisms and mount is minimized, the prisms are cooled down through surrounding He. This provides smooth (better than 0.1° C) temperature distribution across the prisms. Layers of multilayer insulation made of mylar-aluminum foil were wrapped around the internal chamber. A vacuum pump creates a vacuum in the external chamber, further ensuring that the internal chamber remains isolated from the outside environment. Both the internal and external chambers have two fused-silica windows on opposite sides of the chambers, which have sol-gel antireflection coatings.

3.3 Automated Liquid Nitrogen System

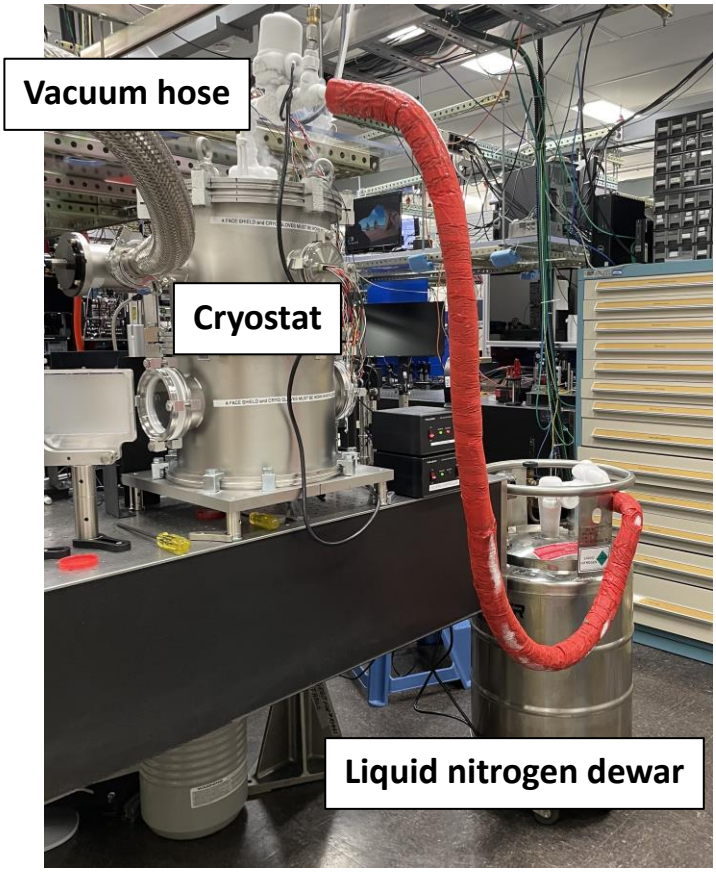

Figure 5: Automated liquid nitrogen filling system. This system was specially designed and fabricated for continuous cooling of the two-chamber cryostat. Liquid nitrogen is pumped from the dewar into the cryostat through a hose, cooling the crystals down from 300 K to 200 K.

An automated liquid nitrogen filling system, shown in Figure 5, was assembled to maintain low temperatures over the full aperture of the KDP and ADP crystals. Vaporized nitrogen creates pressure in the dewar, pushing liquid nitrogen through a hose into the cryostat. A solenoid valve regulates the flow of liquid nitrogen into the cryostat. The system is self-regulating and stops filling when the liquid nitrogen level reaches a set point in the cryostat. A safety valve prevents the pressure inside the dewar from exceeding 35 psi, and an oxygen deficiency detector monitors the oxygen level in the laboratory.

The system was tested to determine how long a dewar of liquid nitrogen will continue pumping before running out. The temperature decreases for about 12 hours when the liquid

nitrogen is filling the cryostat, and then the temperature slowly increases when the liquid nitrogen runs out. A full cycle (room temperature – 200 K – room temperature) lasts around 50 hours.

4 Experiment

Measurements for ADP were done first, and then the cryostat was rotated 180° to make measurements for KDP. The laser beams were precisely directed to hit the ADP crystal at an incidence angle of 8° and the KDP crystal at 12°. Diaphragms, which are opaque structures with an opening in the center, were utilized in the setup in order to keep the beams aligned to the crystals.

As the crystals cooled down from room temperature, around 295 K, to 200 K, the distance the refracted ray moved on a screen was measured for both the ordinary and extraordinary rays of red and green light at different temperatures. From this measurement and Equation (3), the refractive index can be determined at varying temperatures. The screen was located around 8 meters from the prism, making measurements more accurate since the beams are farther apart. The experimental setup was modeled using Graphite software, as shown in Figure 6.

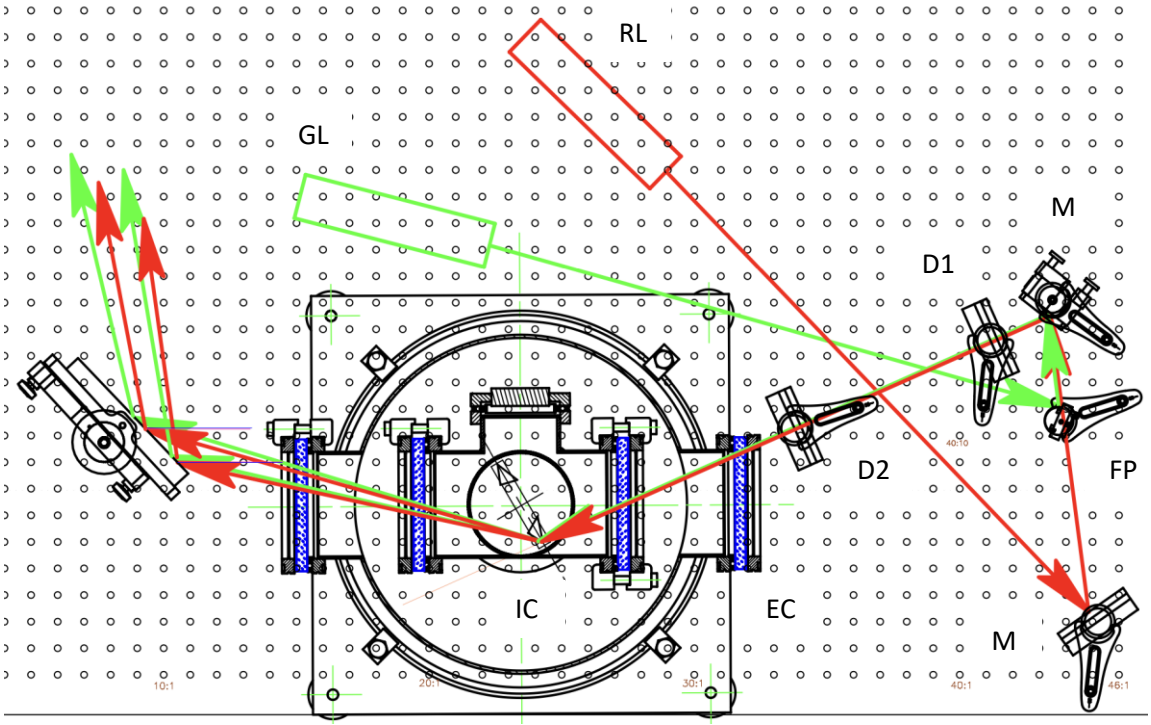

Figure 6: Experimental setup modeled on Graphite software. D1, D2 – input beam alignment diaphragms, M – mirrors, FP – flipping mirror, GL – green laser, RL – red laser, IC – internal chamber, EC – external vacuum chamber

A combination of lenses makes a laser beam collimated. Mirrors align both the red and green beams through the two-chamber cryostat on the same path. A beam enters through a window on the cryostat, passes through the prisms, and exits as two beams through the window on the other side of the cryostat. The two refracted beams then reflect off a mirror and hit a wall where their movements can be tracked. Using this, dimensions of the setup can be measured, and the angle of deviation can be determined.

5 Results

The refractive indices for KDP and ADP were graphed with temperature on the x-axis and refractive index on the y-axis, shown in Figure 7.

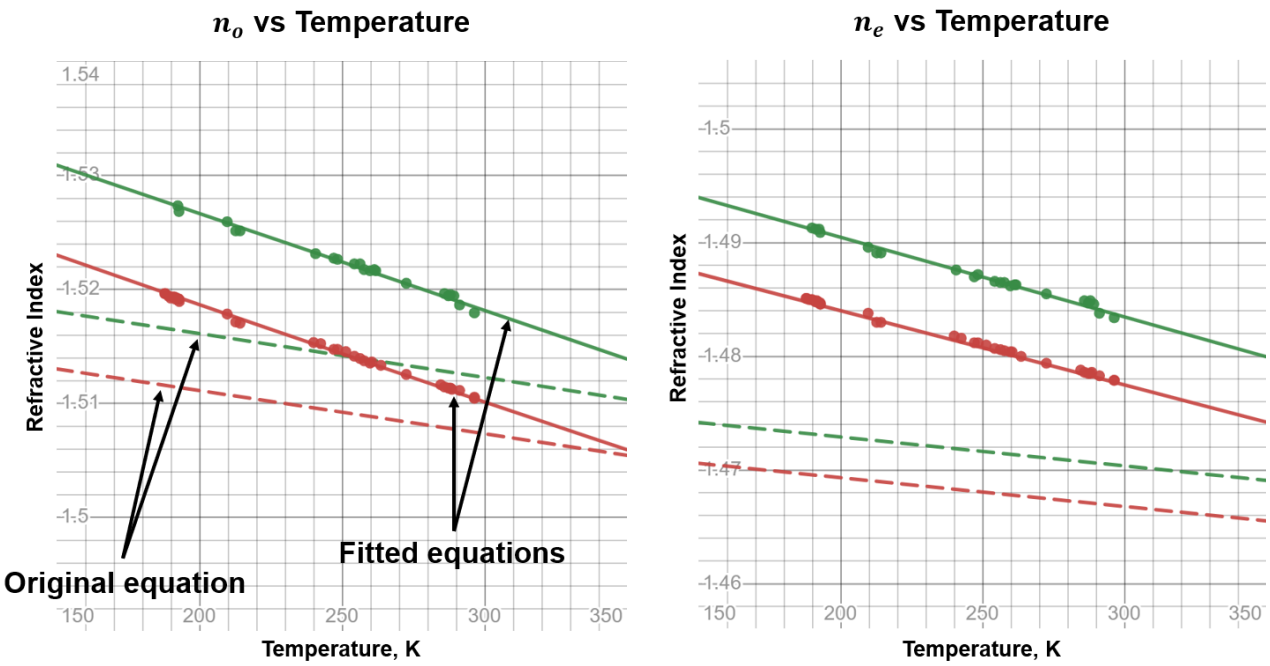

Figure 7: Original and fitted temperature-dependent Sellmeier equations for ordinary and extraordinary beams of KDP. n_o is the ordinary refractive index and n_e is the extraordinary refractive index. The green lines represent the measurements with the green laser and the red lines represent the measurements with the red laser.

The original KDP temperature-dependent Sellmeier equations were modified to fit the new data, with the updated equations shown below.

$$n_o^2 = (1.51 + 3.185 * 10^{-7}T) + \frac{(0.84181 - 1.4114 * 10^{-4}T) * \lambda^2}{\lambda^2 - (0.0139 - 1.83 * 10^{-5}T)} + \frac{(1 + 7.75 * 10^{-3}T) * \lambda^2}{\lambda^2 - 30} \quad (4)$$

$$n_e^2 = (1.495 - 8.2 * 10^{-5}T) + \frac{(0.727 - 1 * 10^{-4}T) * \lambda^2}{\lambda^2 - (0.01513 + 3.104 * 10^{-7}T)} + \frac{(1 - 9.8 * 10^{-4}T) * \lambda^2}{\lambda^2 - 30}$$

Keeping the original form of the equations, the numbers were incrementally adjusted to align the equations with the data points. The modified equations are steeper than the original equations, and there is a clear difference between the original and new graphs.

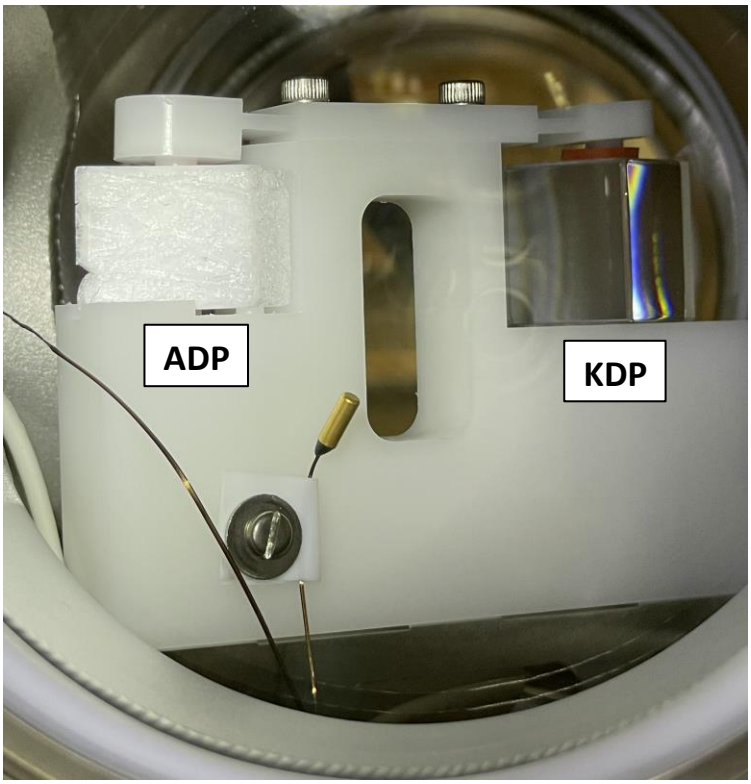

Figure 8: ADP prism cracked and crumbled during cooling stage, blocking any laser light from getting through, while the KDP prism survived.

Unfortunately, the ADP crystal crumbled at around 240 K, as shown in Figure 8. As a result, the data for ADP only ranged from 300 K to 240 K, instead of down to 200 K. One possible reason for this could be an excess amount of moisture inside the crystal, caused by repeated exposure to the air. The moisture in the crystal may have expanded due to the low temperatures, cracking the crystal. Since the ADP crystal cracked and the temperature range is limited, further measurements are needed to get accurate results through a wider range of temperatures.

6 Conclusion

Accurate measurements of the refractive indices of KDP and ADP at varying temperatures are essential to calculate phase matching of a wide range of nonlinear processes. There is a need

to modify the temperature-dependent Sellmeier Equations, which have proved unreliable for many decades.

The refractive indices of KDP and ADP were measured using the deviation of the ordinary and extraordinary beams when passing through triangular prisms at room temperature and at low temperatures. Using a two-chamber cryostat, the temperature could be lowered to 200 K.

A significant discrepancy between the measured refractive indices of KDP and ADP and the refractive indices calculated from the original Sellmeier equations has been demonstrated. The experimentally measured refractive indices at room temperature for KDP and ADP using a room-temperature testbed are in good agreement with the refractive indices calculated from the original Sellmeier equations. However, the same measurements done at room temperature for ADP and KDP inside the cryostat don't line up with the theoretical values from the original Sellmeier equations, showing a systematic error. As a result, additional series of measurements are needed.

7 Acknowledgements

I would like to thank Dr. Ildar Begishev for guiding me through the project. This could not have been done without his dedication and patience. I would also like to thank Alexander Maltsev for cutting and polishing the ADP and KDP prisms, Sean Carey for helping with the sensors and electronics, Mark Romanofsky for designing the prism holder, and Roger Janezic and Salvatore Scarantino for creating the automatic liquid nitrogen filling system. Lastly, I would like to thank Dr. Stephen Craxton for giving me the opportunity to work and do research in this laboratory.

8 References

1. T.R. Boehly, et al., “Initial performance results of the OMEGA laser system,” Opt. Commun. 133, p. 495-506 (1997).

2. J. H. Kelly, et al., “ OMEGA EP: High-Energy Petawatt Capability for the OMEGA Laser Facility,” J. Phys. IV France, **133**, p. 75-80 (2006).

3. J. S. Ross, S. H. Glenzer, J. P. Palastro, B. B. Pollock, D. Price, G. R. Tynan, and D. H. Froula, “Thomson-scattering measurements in the collective and noncollective regimes in laser produced plasmas,” Rev. Sci. Instrum. **81**(10), 10D523 (2010).

4. D. Basting and G. Marowsky, eds., Excimer Laser Technology (Springer, 2005).

5. I.A. Begishev, G. Brent, S. Carey, R. Chapman, I. A Kulagin, M. Romanofsky, M. J. Shoup III, J. D. Zuegel, and J. Bromage, “High-efficiency, fifth-harmonic generation of a joule-level neodymium laser in a large-aperture ammonium dihydrogen phosphate crystal,” Opt. Express, **29**, No. 2, p. 1879-1889 (2021).

6. V.G. Dmitriev, G.G. Gurzaydyan, D.N Nikogosyan, “Handbook of nonlinear optical crystals,” Springer Series in Optical Sciences, vol. 64, Third Edition (1999).